ISBN: 978-3-95450-261-5 ISSN: 2673-7000 doi: 10.18429/JACoW-NAPAC2025-WECN02

EFFECTS OF BEAM CONDITIONS ON ACHIEVING COMPACT LONGITUDINAL DE-CHIRPING USING TRANSVERSE DEFLECTING CAVITIES

A. DeSimone*, G.Ha, Northern Illinois University, DeKalb, IL, USA
S. Doran, W. Liu, J. Power, E. Wisniewski[1], Argonne National Laboratory, Lemont, IL, USA
Q. Marksteiner, H. Xu, N. Yampolsky, Los Alamos National Laboratory, Los Alamos, NM, USA
[1]also at Illinois Institute of Technology, Chicago, IL, USA

Abstract

It has been shown that a transverse deflecting cavity (TDC)-based de-chirper can be made by altering the drift sections in a TDC-based chirper to form negative drifts. While five appropriately configured quadrupole magnets can form such negative drifts, this approach is limited by spatial and experimental constraints. In this study, we investigate an alternative configuration that uses three quadrupole magnets to form a negative identity transport section between the TDCs instead of a negative drift. To assess the robustness of this proposed design, a computational study has been conducted on initial beam conditions to determine operational limitations. This includes the effects of space charge and initial transverse beam conditions, such as beam size and divergence, on the resulting transverse emittance.

INTRODUCTION

A common method for imparting longitudinal chirp to an electron beam is off-crest acceleration in linear accelerator. Slightly off-crest operation causes the head and tail of the bunch to experience different accelerations, which manifests as a longitudinal chirp. Although this method is simple and effective, it inevitably reduces acceleration efficiency, which leads to a lower central beam energy. A novel method was proposed to address this issue so that imparting the chirp does not involve operating the linac off-crest [1].

This method utilizes transverse deflecting cavities (TDCs). TDC, operating at TM_{110} mode, provides a transverse kick based on particles' longitudinal positions and accelerates particles longitudinally based on their transverse positions. Thus, the first TDC introduces a tilt in $z - x$ phase space, then the following TDC provides acceleration based on the horizontal positions of particles, which are correlated to z. In this way, it is possible to impart longitudinal chirp, and the third TDC is introduced to remove remaining unwanted correlations. It is important to note that this configuration only provides negative chirping—head loses energy while tail gains energy—as $\Delta h = R_{65} \propto -\kappa^2$. Ref. [1] also proposed a modification of the beamline to enable dechirping. It could be accomplished by adding five quadrupoles, forming a negative drift section, between TDCs.

Recently a collaboration was initiated to demonstrate the TDC-based chirping and dechirping. While the chirping configuration can be installed at the Argonne Wakefield Accelerator facility [**conde-2017-a**], there is not enough space to accommodate a total of ten quadrupole magnets forming two negative drift sections. Thus, we proposed a new form factor using three quadrupoles forming a negative identity drift [2]. This previous study showed its feasibility. Thus, in this paper, we primarily discuss preliminary study results on limiting factors.

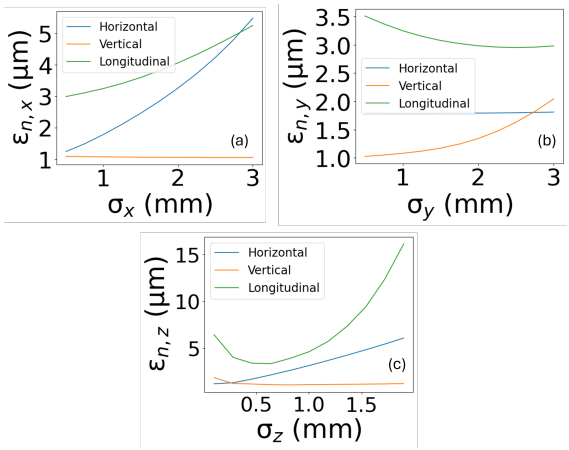

Figure 1: 1D beam size scans.

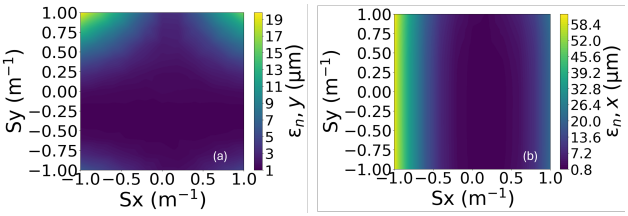

Figure 2: Slope scan results. The phase space slope is defined as $S_x = -\frac{\alpha_x}{\beta_x} = \frac{\langle xx' \rangle}{\langle x^2 \rangle}$.

SIMULATION SETUP

To characterize the beamline's response to various limiting factors, 6D-Gaussian beams were produced and transported in the General Particle Tracer (GPT) code [3]. We scanned beam's second moments at the entrance to find optimal condition minimizing emittance growth and identify

* z2035090@students.niu.edu

ISBN: 978-3-95450-261-5 ISSN: 2673-7000 doi: 10.18429/JACoW-NAPAC2025-WECN02

causes of second-order effects. As the start of the investigation, we applied second-order analysis to the entire dechirper beamline, as well as on space charge effects. The study will be expanded to individual beamline element in future. In addition, a start-to-end simulation was performed to verify the efficacy of the current design.

To find the optimal input beam condition for a de-chirper with negative identity sections, initial slopes (S_x, S_y, S_z) and beam sizes (σ_x, σ_y, σ_z) were scanned, and the final normalized emittances in each plane were estimated. In these simulations, the quadrupoles had hard edges and the effective length of 0.12 m. Their geometric strength was $1\,\mathrm{T}\cdot\mathrm{m}^{-1}$. CST-modeled TDC field maps were imported for the simulation [4]. It had a width of approximately 0.3 m, and each TDC used strengths of $1.7\,\mathrm{m}^{-1}$, $3.4\,\mathrm{m}^{-1}$, and $1.7\,\mathrm{m}^{-1}$, respectively. Note that these strengths approximately correspond to RF powers of 2.5, 10, and 2.5 MW.

ANALYSIS OF EMITTANCE GROWTH IN A DECHIRPER

Emittance Dependence on Incident Conditions

Figures 1 and 2 shows the final emittances as a function of incident second moments. When specified variables are scanned, other variables were fixed to the values in Table 1, which have been optimized.

Both results show clear nonlinear dependence of emittances on the second moments, which is an evidence of strong second order effects. The growth can be minimized when the second moments are close to the values in Table 1. One important observation is that σ_y and σ_z have optimum around 1.5 mm and 0.5 mm, respectively while a smaller σ_x is always preferred. This could be related to space charge effects in the beamline.

Table 1: Optimal Incident Beam Conditions

Parameters	Values
$\varepsilon_{\mathrm{n},x}$, $\varepsilon_{\mathrm{n},y}$	1 µm
σ_x, σ_y	1 mm
σ_z	0.5 mm
S_x	$0.2\,\mathrm{m}^{-1}$
S_y	$-0.2\,\mathrm{m}^{-1}$
S_z	$-6\,\mathrm{m}^{-1}$

Second-Order Effect Analysis

To count the higher-order effects originating from TDC field maps, a crystal lattice-like particle array in 6D phase space was sent through the dechirper. From these initial and final distribution, second-order transfer matrix can be calculated using,

$$T = (\mathbf{X}_f\mathbf{X}_i^T)(\mathbf{X}_i\mathbf{X}_i^T)^{-1}, \quad (1)$$

where $\mathbf{X} = (x, x', y, y' z, \delta)^T$.

While the calculated matrix components show candidates for strong contributions, the actual second order effects need to evaluate beam contribution and cancellation between second-order terms. Thus, an ideal particle distribution was generated. Then, we grouped and calculated second-order terms' magnitudes.

In total, there will be six groups of second-order terms for each final coordinate. In-plane groups' magnitude was calculated by,

$$\langle(\mathrm{T}_{ijj}X_jX_j + \mathrm{T}_{ij(j+1)}X_jX_{j+1} + \mathrm{T}_{i(j+1)(j+1)}X_{j+1}X_{j+1})^2\rangle, \quad (2)$$

where $i \in \{1,2,3,4,5,6\}$ and $j \in \{1,3,5\}$. Similarly, for the cross-plane groups,

$$\langle(T_{ijk}X_jX_k + T_{ij(k+1)}X_jX_{k+1} + T_{i(j+1)k}X_{j+1}X_k + T_{i(j+1)(k+1)}X_{j+1}X_{k+1})^2\rangle, \quad (3)$$

where $j,k \in \{1,3,5\}$ and $j \neq k$.

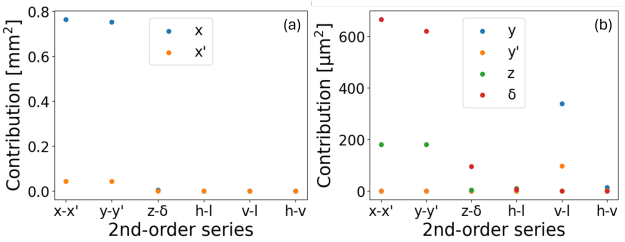

Figure 3: Contributions of second order groups on final particle coordinates. 'h', 'v', and 'l' correspond to horizontal, vertical, and longitudinal, respectively.

Figure 3 compares the magnitude of each group for the final beam coordinates. The largest aberrations are on the final x-coordinate, and contributions from the $x - x'$ and $y - y'$ second-order groups are dominant. This result also indicates that the term could be easily minimized by adjusting the incident slope since the terms within the group can cancel each other. Further investigation will be required to identify the actual source in the beamline and understand the dynamics better.

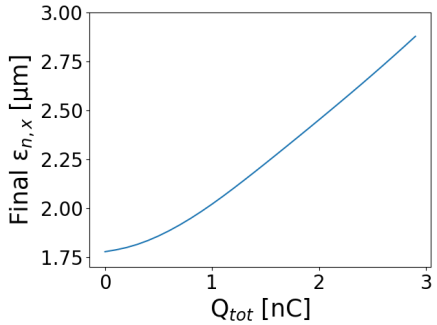

Figure 4: Spacecharge effects on horizontal emittance.

ISBN: 978-3-95450-261-5 ISSN: 2673-7000 doi: 10.18429/JACoW-NAPAC2025-WECN02

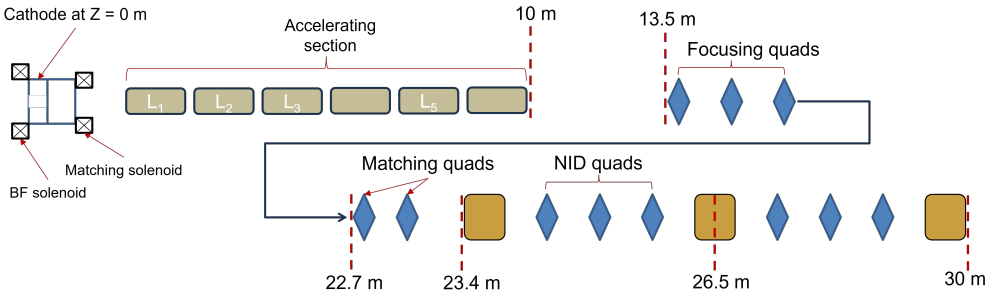

Figure 5: Proposed AWA dechirper beamline.

SPACE CHARGE EFFECTS

While the space charge effect is usually not a concern for 100 pC beam with the energy of 44 MeV, negative identity section includes a strong focusing in the plane of interest. Thus, it could introduce horizontal emittance growth. To characterize these effects, simulations were conducted with various bunch charges. Again, a 6D Gaussian beam was adopted for this test.

The simulation results are shown in Fig. 4. As expected, the space-charge effect increases the final horizontal emittance. When the use of high-charge beam is necessary, further adjustment of transverse optics will be required. However, it is worth noting that the growth is tolerable for low charges such as 100 pC.

START-TO-END SIMULATION

Considering the beam conditions found from the parameter scans, a start-to-end simulation was conducted to verify the efficacy of the proposed dechirper. The beamline layout (including the dechirper) and simulation results are shown in Fig. 5 and Fig. 6. The launching phase of the gun was set to 50°, which provided maximum energy gain. Linac phase was set to 0 ° (on-crest). The beamline includes two sets of solenoids near the gun, providing bucking-focusing and matching, with currents set to 550 A and 203 A, respectively, to provide a good transverse emittance and reasonable beam size to match into the dechirper beamline. There are two sets of quadrupoles that provide further focusing and matching into the dechirper. These quadrupoles were set to -0.4, 1.2, -0.4 T/m and 0.96, -0.6 T/m, respectively.

The initial and final longitudinal phase spaces, shown in Fig. 6, demonstrate successful control of the longitudinal chirp. While further optimization is required, the emittance growth has been mitigated through the dechirper. At the entrance of the dechirper, emittances were $\{\varepsilon_{n,x}, \varepsilon_{n,y}, \varepsilon_{n,z}\}$ = 0.8 µm, 0.9 µm, and 12 µm; at the exit of the dechirper, 1.5 µm, 1 µm, and 19 µm.

FUTURE WORK

Although the second-order effects were observed and their contributions were estimated, it remains to be seen exactly where in the dechirper these effects originate. In the rest of 2025, the beamline design for the dechirper experimental demo will be finalized, and a cold test of TDCs will be conducted. We plan to commission the the TDCs and install the dechirper during the first half of 2026.

ACKNOWLEDGMENT

This research is supported by the U.S. Department of Energy through the Laboratory Directed Research and Development program of the Los Alamos National Laboratory under project number 20240231ER and the Department of Energy, Office of High Energy Physics, under Contract No. DE-AC02-06CH11357.

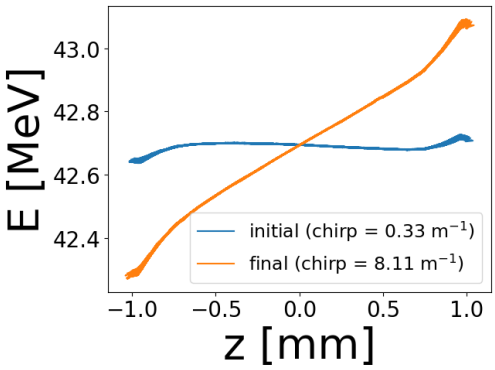

Figure 6: Longitudinal phase spaces before and after the dechirper.

REFERENCES

[1] N. Yampolsky, E. I. Simakov, and A. Malyzhenkov, "Imposing strong correlated energy spread on relativistic bunches with transverse deflecting cavities", *Phys. Rev. Accel. Beams*, vol. 23, no. 5, p. 054 403, May 2020. doi:10.1103/physrevaccelbeams.23.054403

[2] A. DeSimone *et al.*, "Design study for a transverse deflecting cavity based de-chirper", Taipei, Taiwan, May 2025, paper TUPM015, to be published.

[3] M. J. de Loos and S. B. van der Geer, "General Particle Tracer: A 3D Code for Accelerator and Beam Line Design", in *Proc. EPAC'98*, Stockholm, Sweden, pp. 1245–1247, 1998. https://jacow.org/e98/papers/THP18F.pdf

[4] P. Piot *et al.*, "Commissioning of a 1.3-GHz Deflecting Cavity for Phase-Space Exchange at the Argonne Wakefield Accelerator", in *Proc. IPAC'12*, New Orleans, LA, USA, May 2012, pp. 3350–3352. https://jacow.org/IPAC2012/papers/THPPC031.pdf